

## Role of Threaded Tool Pin Profile and Rotational Speed on Generation of Defect Free Friction Stir AA 2014 Aluminium Alloy Welds

Suresh D. Meshram<sup>\*,\*</sup>, G. Madhusudhan Reddy<sup>#</sup>, and A. Venugopal Rao<sup>#</sup>

<sup>#</sup>Defence Metallurgical Research Laboratory, Hyderabad - 500 058, India

<sup>\*</sup>E-mail: suresh\_uor@yahoo.co.in

### ABSTRACT

Influence of threads on tool pin and rotational speeds on defect occurrence in friction stir welding (FSW) of aluminum alloy AA 2014 T6 plates has been studied. The effect of FSW forces on the evolution of mechanistic defects, caused in turn through a variation in heat generation during the process has also been examined. In case of conical tool pin, relatively lower rotational speeds resulted in unbounded zones and micro defects while high speeds caused excessive flash, thereby resulting in surface defects and voids inside the weld. The FSW joints were defect-free at moderate speeds, hinting an optimum heat generation and flow. Reaction forces on the tool pin, in the welding direction, were correlated with the defect formation. Tools equipped with a threaded conical pin profile resulted in sound welds, irrespective of the tool rotational speeds in the entire range of 400 rpm - 2400 rpm. The threaded conical pin, with a relatively larger frictional area, may be contributing to higher levels of heat generation compared to a plain conical pin. Further, positive displacement of the hot plasticised material by the threads will carry away excess heat from the advancing-to-the-retracting side and simultaneously downwards, thus confining all heat within the weld zone.

**Keywords:** Frictions stir welding, rotational speed, aluminum alloy, conical tool pin

### 1. INTRODUCTION

Friction stir welding (FSW) is a relatively new, solid-state welding process, characterised by localised thermo-mechanical phenomena. It has emerged as a candidate process for the successful welding of aluminum alloys that were previously described as not weldable (2xxx series and 7xxx series)<sup>1</sup>. The FSW process and its terminology are schematically illustrated in Fig. 1. The important process parameters in FSW are the tool geometry, axial force, rotational speed, traverse speed and, tool tilt angle<sup>1</sup>.

Many studies have been carried out on the FSW of precipitation hardenable and non heat-treatable aluminium alloys. These studies are mainly focused towards microstructural characterisation<sup>1-4</sup> and effect of welding parameters on mechanical properties<sup>5-7</sup>. Role of welding parameters on hardness, fatigue strength, residual stress and microstructural evolution has also been studied by many researchers<sup>1,3,4,8,9</sup>. In any process such as FSW, involving complex thermo-mechanical phenomena, the interaction between material and process variables determines the achievable process goals. In spite of large amount of published work on role of tool pin profile in producing defect-free joints<sup>10-13</sup>, the influence of tool pin profile has not been meticulously correlated with force/torque acting on tool.

In analysing the mechanics of friction-stir welding and processing (FSW/P), researchers have employed experimental and numerical techniques to study the flow and consolidation of materials under the shoulder. Many flow visualisation

studies<sup>14,15</sup> and numerical analyses<sup>16</sup> have been performed in an effort to understand the material flow behaviour. An examination of the process forces associated with the plastic flow around the tool can provide valuable insights in improving the level of understanding and control of the FSW process. The process signatures created by varying the FSW/P variables can bring out the working mechanism of FSW/P.

Hattingh<sup>17</sup>, *et al.* analysed the force footprints to systematically study the influence of tool geometry on FSW process parameters and on weld tensile strength, in an effort to optimize the tool design thereby producing welds with 97 per cent of the parent metal strength in Al 5083-H321 alloy. Studies on the relationship between tool profiles, rotational speeds, traverse speed and the microstructure using force footprint plots were reported by Hattingh<sup>18</sup>, *et al.* Arbegast<sup>19</sup> experimentally demonstrated the influence of clamping locations, welding direction, crossing over pre-existing FSW and the process parameters (such as rotation rate and traverse speed) on the measured tool forces.

The main thrust of research in FSW of heat treatable Al-alloys has been directed towards the joining of alloys such as AA 2024, AA 2195, AA 6061 and AA 7075<sup>20,21</sup>. FSW of aluminum alloy AA 2014 is the focus of the present investigation, in view of its widespread applications in the aircraft industry<sup>22</sup>. Other applications include; military vehicles, bridges, weapons manufacture and structural applications.

The tendency for hot cracking during solidification is the most important factor governing the weldability of 2xxx series

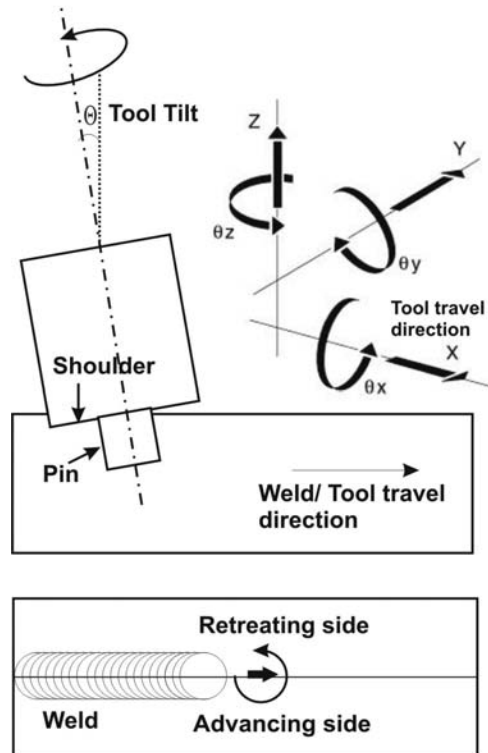


Figure 1. Schematic view of friction stir welding process with nomenclature.

Al-alloys. The susceptibility to solidification cracking during fusion welding is governed by the composition of the weld pool. Additionally, the weld fusion zone typically exhibits coarse columnar grains because of the prevailing thermal conditions during solidification in the weld pool. This often leads to inferior mechanical properties and poor resistance to hot cracking in the weld joint. This problem in fusion welding can be eliminated by adopting FSW, which being a solid-state process does not involve melting/ solidification related issues. Among the FSW process parameters, tool rotational speed is one of the most important variables, since it plays a major role in the heat generation which in turn controls the metallurgical and mechanical properties of the weld<sup>23</sup>.

In this investigation, an attempt has been made to understand the effect of tool pin profile and rotational speed on the weld quality of AA 2014 aluminum alloys using the FSW process. Plain conical pin and threaded conical pin are the tool pin profiles investigated in this study. Different tool rotational speeds were used with the two tool pin profiles, keeping the other parameters such as tool tilt angle ( $2^\circ$ ), tool travel speed (50 mm/min) and plunge depth (5.7 mm) constant. Appearance of the weld for different tool rotational speeds is examined and the impact of tool pin profile on defect formation, material flow, reaction forces on the tool pin during FSW of AA 2014 is studied.

## 2. EXPERIMENTAL PROCEDURE

Rolled plates of 6 mm thickness of AA 2014 in T6 condition, with chemical composition as given in the Table 1, were cut into the required size (75 mm x 150 mm) with square butt configuration to fabricate the FSW joints. Hot rolled die

steel (AISI-H13), with a chemical composition given in Table 2, was used as the tool material.

An indigenously designed and developed FSW machine (50 kN, 2400 rpm, position controlled) was used to fabricate the joints. Two pin tools used for welding had similar dimensions with the exception that one tool had threads on pin (Fig. 2). Plunge depth was maintained constant at 5.7 mm.

Table 1. Chemical composition of AA 2014 Al alloy

Element	Cu	Mn	Si	Mg	Al
Wt%	4.2	0.8	0.8	0.5	Bal.

Table 2. Chemical composition of hot worked die steel (AISI-H13)

Element	C	Cr	V	Mo	Si	Fe
Wt%	0.30	5.13	1.0	1.33	1.00	Bal.

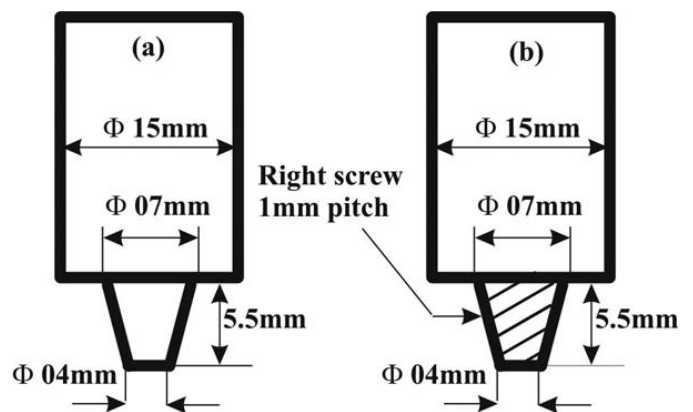


Figure 2. Schematic view of tool used: (a) Conical tool, (b) Conical threaded tool.

The square butt joint configuration was produced by securing the plates in position using mechanical clamps. Keeping the direction of welding normal to the rolling direction, friction stir welds were made at different tool rotational speeds ranging from 400 rpm to 2400 rpm (in intervals of 200 rpm), for each of the two tool pin profiles. The other process parameters such as travel speed (50 mm/min) tool tilt angle ( $2^\circ$ ) were kept constant.

The reaction forces on the tool in the direction of tool travel (X-axis force) and along the spindle axis (Z-axis force) recorded, through a multi-axis sensor attached to the spindle head that can determine the loading on the tool by measuring the forces and torque along the three orthogonal axes. The transverse section of each of the welds were mounted and polished as per standard procedure and etched with Keller's reagent to reveal the macro- and microstructures. Defect size is measured by outlining the defect area as observed in optical microscopy in adobe pdf professional software, which calculates the outline area. Three different locations in a weld is analysed and average of it is reported.

## 3. RESULTS AND DISCUSSION

### 3.1 Plain Conical Tool Pin Profile

The top surface images (crown surface) of the weld zone,

obtained using various tool rotational speeds are presented in Fig. 3. Rotational speeds ranging from 400 rpm to 2400 rpm were used in the experiments. The top region of weldments revealed no surface defects at tool rotational speeds below 1400 rpm. However, at speeds above 1400 rpm, line defects were found to occur.

Low magnification images of the weld zone cross-section, shown in Fig. 4, display features of defect formation at various tool rotational speeds. The weld zones shown in Figs. 4(a) to 4(c) display the unbounded region on the retreating side, which is the transition zone between the stirred and thermo-mechanically affected zones (TMAZ) for the tool rotational speeds in the range 400 rpm - 800 rpm. This region forms the interface between the undeformed parent metal and the plasticised weld-zone during tool translation. Formation of the unbounded region at lower rotational speeds (400 rpm to 800 rpm) could be related to the relatively lower heat input which in turn leads to inadequate plasticity confined to the immediate vicinity of the pin<sup>24</sup>. Also, the progressive decrease in the size of the observed voids for rotational speeds up to 800 rpm may be attributed to the increased stirring action due to relatively higher levels of heat generation<sup>1,24</sup>.

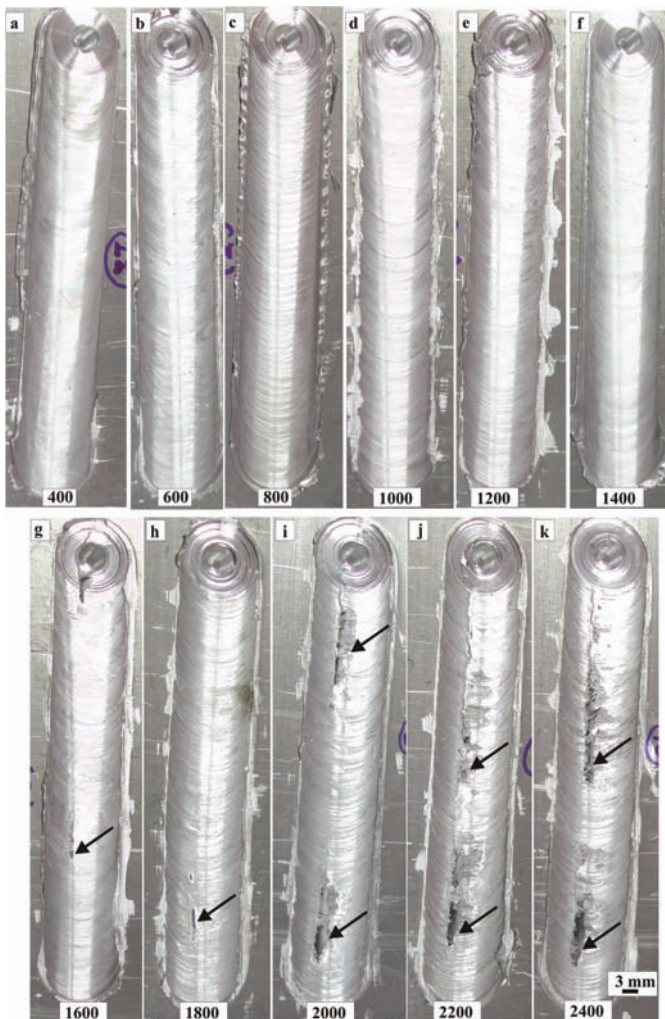


**Figure 3.** Top surface images of the weld zone with various tool rotation speeds from (a) 400 rpm to (k) 2400 rpm for conical tool (Arrow indicates line defects).

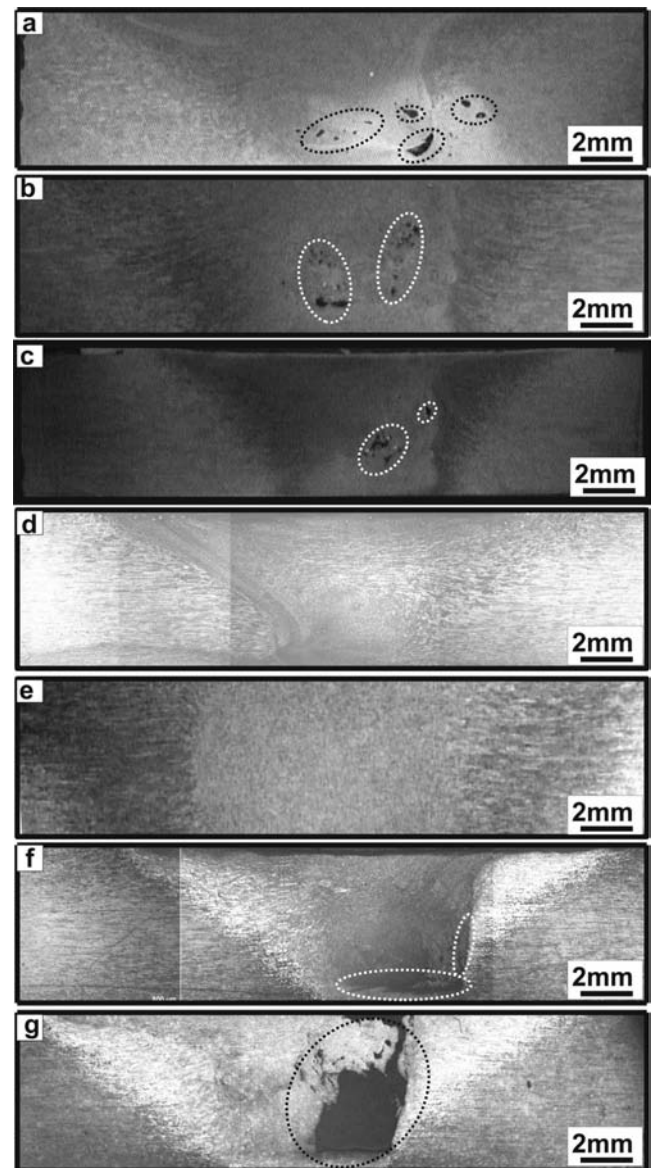


**Figure 4.** Macro view of the cross section of welds with conical tool at: (a) 400 rpm, (b) 600, (c) 800 rpm, (d) 1000 rpm, (e) 1200 rpm, (f) 1400 rpm, and (g) 2400 rpm.

Line defects and large tunneling voids were observed for tool rotational speeds above 1200 rpm. These voids might have formed because of the movement of an excessive amount of stirred material to the upper surface of the weld region. Also, the observed defects in weldments at higher rotational speeds may be due to understandably high temperature leading to the tool losing control over the material movement around the pin i.e. material is not confined with the tool since turbulent/unstable flow of material takes place at high rotational speed due to high temperature and high velocity. It is well documented in the literature that higher rotational speeds increase the temperature of the material due to higher relative velocity at the tool-workpiece interface and consequently a faster rate of heat generation<sup>25</sup>. This ultimately causes a reduction in the flow stress of the material below the shoulder, surrounding the pin. Higher heat input can improve the flow of the plasticised material<sup>3,24</sup>, as evidenced by the defect-free welds produced



with tool rotation speeds between 1000 rpm and 1200 rpm. This points to the existence of a rather narrow welding parameter envelop for production of sound welds by FSW.

The results can be explained further through the observed trends in the tool pin reaction forces, with the variation in tool rotational speeds. The reaction force on the tool opposite to the weld direction, which is also called the X-axis force, is one of the important output parameters in FSW. This force is a key indicator of the patterns of metal flow in FSW. The force decreases with increasing rotational speeds up to 1000 rpm, indicating enhanced plasticity in the stirred region. This is consistent with the observed decrease in void defects with increasing rotational speeds up to 1000 rpm as shown in Fig. 5.

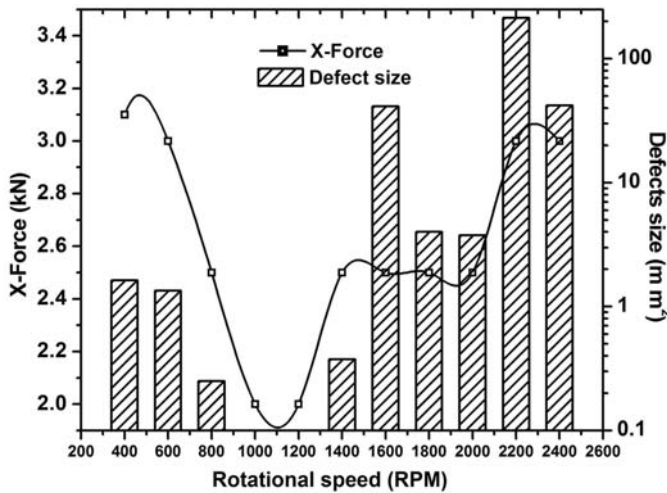


Figure 5. Variation in force and defect with respect to rotational speed for a conical tool.

This observation of minimum opposing force on tool pin coupled with nil defects continues in the tool rotational speed range 1000 rpm to 1200 rpm. With increasing rotational speed the heat generation in the plate surrounding the pin increases and hence the material becomes soft till the speed reaches the range of 1000 rpm to 1200 rpm resulting low X-force. Beyond 1200 rpm, the force registered a steep increase. The likely rapid increase in the volume of stirred material around the pin, with increasing rotational speeds beyond 1200 rpm, may be causing a steep increase in the tool reaction force due to the need to displace a large volume of stirred material. This observation is also strengthened by the conspicuous oscillations in the recorded tool force at higher rotational speeds as shown in Fig. 6. This also suggests that as the tool reaction force curve fluctuates with high frequency, there is a greater likelihood of more surface defects developing.

The value of X-axis force fluctuates between high and low values. The X-axis force and torque peaks are nearly in-phase however fluctuation in the amplitude of X-force is much higher compared to that of the torque<sup>14</sup> as shown in Fig. 7.

Based on the above results, it may be summarised that the weld pitch (tool travel speed/rotational speed) plays a major role in the production of sound welds. An optimum weld pitch has to be determined, by adopting a trial-and-error approach to experiments involving different combinations of tool rotational and travel speeds<sup>26</sup>.

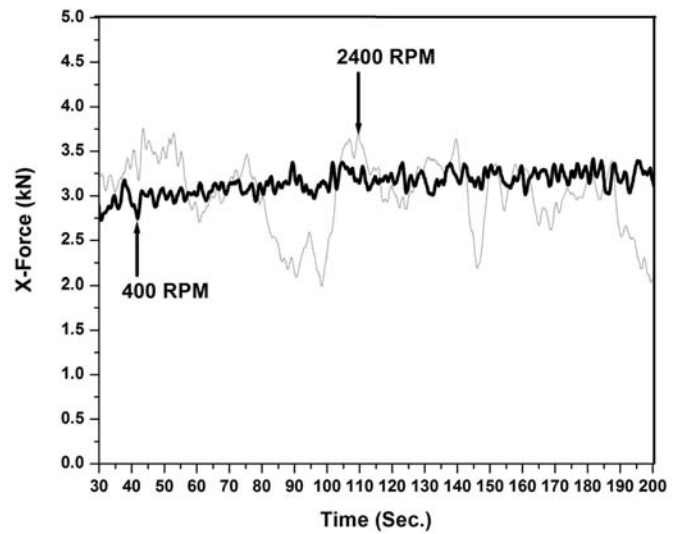


Figure 6. Variation of X-force with respect to time for welds at 400 rpm and 2400 rpm for a conical tool.

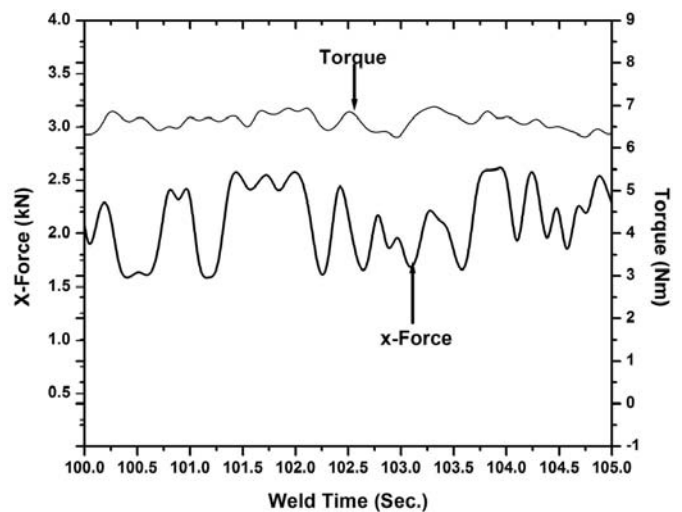
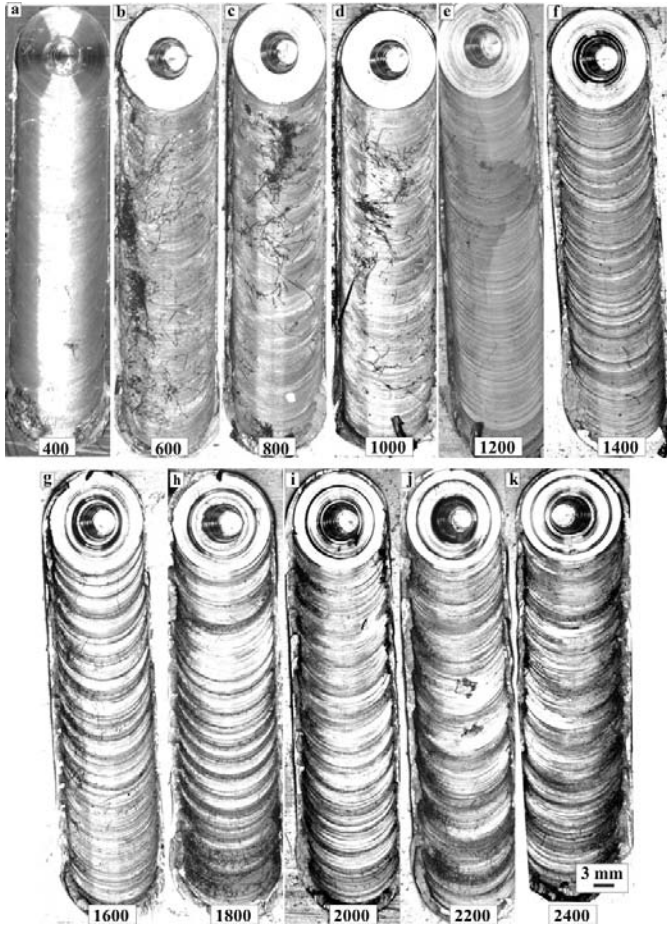


Figure 7. Showing variation of the torque and the X-force as the function of time along the welding path at 1000 rpm for a conical tool.

### 3.2 Conical Tool with Thread

Figures 8 and 9, respectively represent the top surface image (crown surface) and cross-section of the weld zone, obtained at different tool rotational speeds with a fixed welding speed of 50 mm/min. The tool rotational speeds ranged from 400 rpm to 2400 rpm. All the joints are free from defects like pin holes, tunnels, cracks etc. This shows that the consolidation of weld metal is uniform and good in friction-stir processing (FSP) region for all joints. Even though the FSP zone is free from defects, its shape and dimensions are different in each case. Top surface of the weld with rotational speed 1400 rpm to 2400 rpm shows rough surface as compared to weld with low rpm. Reduction in flow strength of weld metal at high temperature, due to high rotational speed can be attributed to the formation of rough surface. This configuration (conical pin with thread) of the tool may be promoting a higher level of hydrostatic stress along the joint causing a better consolidation of the plasticised material. The higher level of plasticisation



**Figure 8.** Top surface images of the weld zone with various tool rotation speeds from (a) 400 rpm to (k) 2400 rpm for conical threaded tool.

in the work-piece material is due to greater amount of heat generation resulting from a relatively larger frictional area of threaded pin as compared to a smooth conical tool. This can be explained based on the observed forces on the tool pin. Figures 10 and 11, respectively show a variation of the in-plane force ( $F_x$ ) and downward forging force ( $F_z$ ), for various rotational speeds by the conical tool pin with and without thread.

It may be observed from Figs.10 and 11 that irrespective of the tool rotational speeds, both  $F_x$  and  $F_z$  forces are relatively lower for the threaded tool, compared to those recorded for the smooth conical tool pin. This indicates that the threaded tool profile generates a relatively localised deformation, as compared to that by the smooth conical tool pin, which in turn results in a decrease in the traverse force and forging force. Localised deformation results in higher rate of heat generation in a small area surrounding the pin where extensive deformation has occurred. This makes the material soft enough to be carried along with the pin and filling up the voids which would have been formed otherwise, if rate of heat generation is low. Low rate of heat generation (in absence of localised deformation) results more area of TMAZ i.e. more volume of material stirred and carried with the pin tool, not heated up sufficiently, resulting in voids. Threaded pins were found to assist in ensuring that the plastically deformed material is fully delivered around the pin, apart from causing a free mixing of

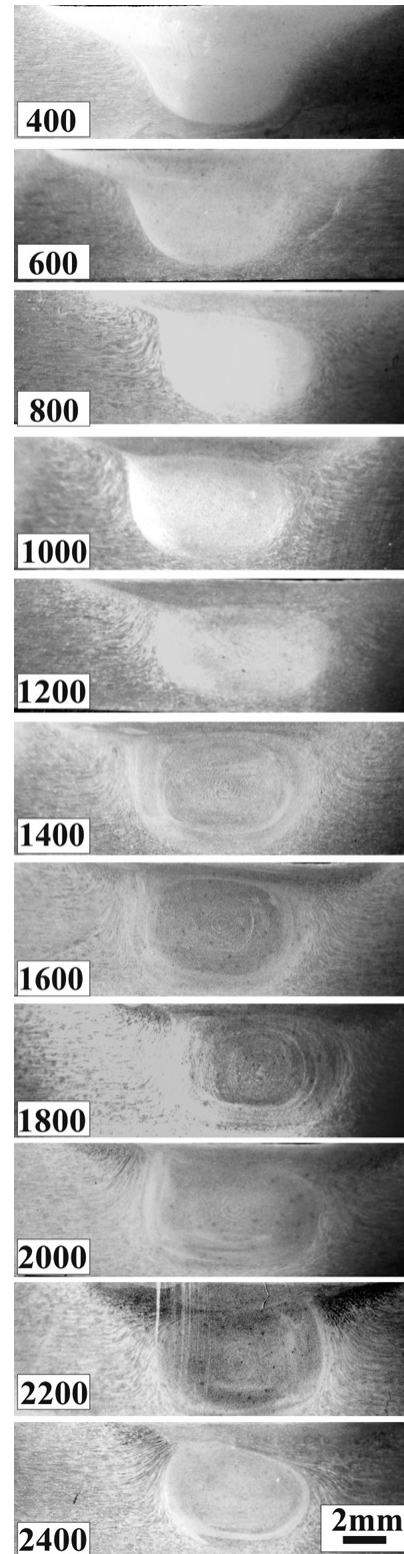


**Figure 9.** Macro view of the cross section of the welds with conical threaded tool at different rpm.

the material between the upper and lower parts of the weld joint. This enhanced mixing in turn enables the use of higher speeds in FSW, ultimately leading to faster, better quality, and void-free welds. The enhanced mixing enabled by the threaded pin will also allow the usage of higher weld traverse speeds, which results in reduced softened/heat affected zone (HAZ)



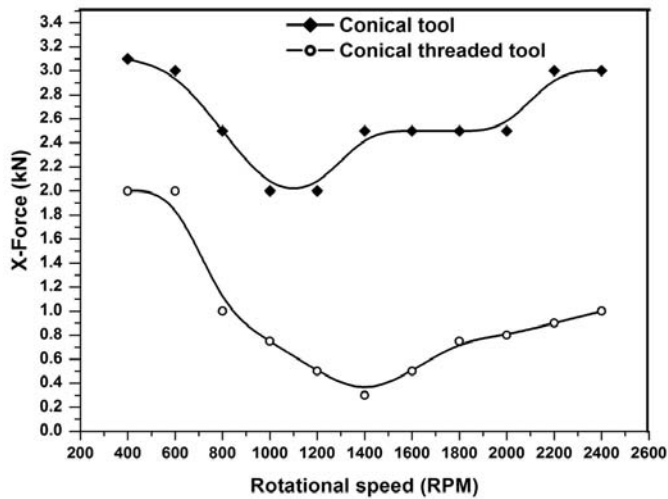


Figure 10. Variation of X-Force for conical and conical threaded tool with different rpm.

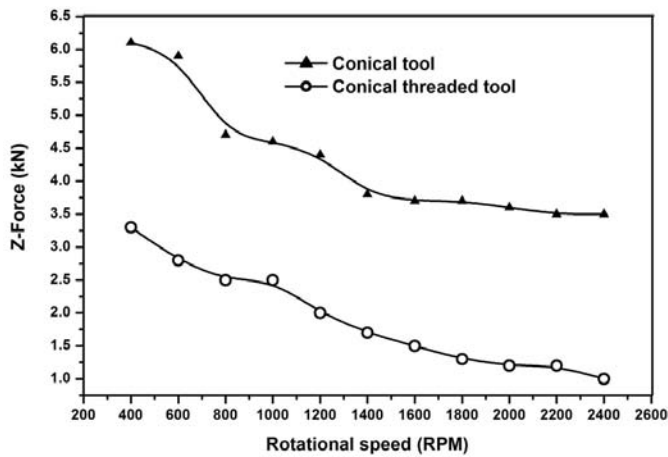


Figure 11. Variation of Z-Force for conical and conical threaded tool with different rpm.

which obviously helps in generation of better mechanical properties. The present experiments have demonstrated that the conical tool pin with threaded profile is more effective in producing sound welds over a wide range of FSW parameters.

#### 4. CONCLUSIONS

A study of the influence of tool rotational speeds in friction stir welding of Aluminum alloy AA 2014 T6 has brought out its significance on defect formation/elimination, apart from the trends in transverse and axial reaction forces on the tool. The major observations emerging from this work are as follows:

- (i) Plain conical tool pin results in lower levels of frictional heating at slow rotational speeds (400 rpm - 800 rpm), resulting in sluggish movement of material around the pin and consequent defects in the form of voids and unbounded region. This is accompanied by a decrease in X-direction reaction force with increasing speeds, due to the plastic softening and stirring of the material in the weld zone.
- (ii) Higher rotational speeds with unthreaded conical pin cause excessive surface heating and chaotic metal flow, leading to large surface/sub-surface defects. At very high tool

rational speeds, the X-direction reaction force increases steeply, probably due to movement of an excessive amount of stirred material at the upper surface of the weld region. Plain conical pin was yielding defect-free welds in a narrow speed range of 1000 rpm - 1200 rpm.

- (iii) In comparison, the conical pin with threads results in consistently lower X-direction reaction and axial forces. The average temperatures in the weld zone may be relatively higher due to the increased frictional area (of the threads) and the rapid plastic deformation imparted by the threads. Also, the threaded pin causes positive displacement of the plasticised material from the advancing to the retreating side and simultaneously downwards, thereby removing the heat from the weld zone from time-to-time apart from confining it to a narrow band along the weld.

#### REFERENCES

1. Jata, K.V.; Sankaran, K.K. & Ruschau, J.J. Friction stir welding effects on microstructure and fatigue of aluminium alloy 7050-T7451. *Metall. Mater. Trans. A*, 2000, **31**(9), 2181-2192. doi: 10.1007/s11661-000-0136-9.
2. Su, J.Q.; Nelson, T.W.; Misra, R. & Mahoney, M. Microstructural investigation of friction stir welded 7050-T651 aluminium. *Acta Mater.*, 2003, **51**(3), 713-729. doi: 10.1016/S1359-6454(02)00449-4.
3. Sato, Y.S.; Park, S.H.C. & Kokawa, H. Microstructural factors governing hardness in friction-stir welds of solid-solution-hardened Al alloys. *Metall. Mater. Trans. A*, 2001, **32**(12), 3033-3042. doi: 10.1007/s11661-001-0178-7.
4. Sato, Y.S.; Urata, M. & Kokawa, H. Parameters controlling microstructure and hardness during FSW of precipitation-hardenable aluminium alloy 6063. *Metall. Mater. Trans. A*, 2002, **33**(3), 625-635. doi: 10.1007/s11661-002-0124-3.
5. Liu, H.; Maeda, M.; Fujii, H. & Nogi K. Tensile properties and fracture locations of friction-stir welded joints of 1050-H24 aluminum alloy. *J. Mater. Sci. Lett.*, 2003, **22**(1), 41-43. doi: 10.1023/A:1021726123864.
6. Liu, H.J.; Fujii, H.; Maeda, M. & Nogi K. Tensile properties and fracture locations of friction-stir-welded joints of 2017-T351 aluminum alloy. *J. Mater. Process. Technol.*, 2003, **142**(3), 692-696. doi:10.1016/S0924-0136(03)00806-9.
7. Liu, H.; Fujii, H.; Maeda, M. & Nogi, K. Tensile properties and fracture locations of friction-stir welded joints of 6061-T6 aluminum alloy. *J. Mater. Sci. Lett.*, 2003, **22**(15), 1061-1063. doi: 10.1023/A:1024970421082.
8. Peel, M.; Stenwex, A.; Preuss, M. & Withers, P.J. Microstructure, mechanical properties and residual stresses as a function of welding speed in aluminum AA5083 friction stir welds. *Acta Mater.*, 2003, **51**(16), 4791-4801. doi:10.1016/S1359-6454(03)00319-7.
9. James, M.N.; Hattingh, D.G. & Bradley, G.R. Weld tool

- travel speed effects on fatigue life of friction stir welds in 5083 aluminium. *Int. J. Fatigue*, 2003, **25**(12), 1389–1398. doi:10.1016/S0142-1123(03)00061-6.
10. Baskoro, A.S.; Suwarsono,; Kiswanto, G. & Winarto. Effects of high speed tool rotation in micro friction stir spot welding of Aluminum A1100. *Appl. Mech. Mater.*, 2014, **493**, 739-742. doi: 10.4028/www.scientific.net/AMM.493.739.
  11. Buffa, G.; Fratini, L.; Schneider, M. & Merklein, M. Effect of process parameters on the joint integrity in friction stir welding of Ti-6Al-4V lap joints. *Key Engg. Mater.*, 2013, **554-557**, 1083-1090. doi: 10.4028/www.scientific.net/KEM.554-557.1083.
  12. Ramulu, P.J.; Narayanan, R.G.; Kailas, S.V. & Reddy, J. Internal defect and process parameter analysis during friction stir welding of Al 6061 sheets. *Int. J. Adv. Manuf. Technol.*, 2013, **65**(9-12), 1515-1528. doi: 10.1007/s00170-012-4276-z.
  13. Abdel-Gwad, E.F.; Shahenda, A. & Soher, S. Effect of friction stir welding parameters on thermal and tensile behaviour of aluminum weldments using double shoulder tools. *Adv. Mater.Res.*, 2013, **622-623**, 323-329. doi: 10.4028/www.scientific.net/AMR.622-623.323.
  14. Reynolds, A.P. Flow visualisation and simulation in friction stir welding. *Scripta Mater.*, 2008, **58**(3), 338-342. doi:10.1016/j.scriptamat.2007.10.048.
  15. Schmidt, H.N.B; Dickerson, T.L. & Hattel, J.H. Material flow in butt friction stir welds in AA2024-T3. *Acta Mater.*, 2006, **54**(4), 1199-1209. doi:10.1016/j.actamat.2005.10.052.
  16. Colegrove, P.A. & Shercliff, H.R. 3-Dimensional CFD modelling of flow around threaded friction stir welding tool profile. *J. Mater. Process. Technol.*, 2005, **169**(2), 320–327. doi:10.1016/j.jmatprotec.2005.03.015.
  17. Hattingh, D.G.; Blignault, C.; Niekerk, T.I. van. & James, M.N. Characterisation of the influences of FSW tool geometry on welding forces and weld tensile strength using an instrumented tool. *J. Mater. Process. Technol.*, 2008, **203**(1-3), 46-57. doi:10.1016/j.jmatprotec.2007.10.028.
  18. Hattingh, D.G.; Niekerk, T.I. van.; Blignault, C.; Kruger, G. & James, M.N. Analysis of the FSW force footprint and its relationship with process parameters to optimise weld performance and tool design. *Weld. World*, 2004, **48**(1-2), 50-58. doi: 10.1007/BF03266414.
  19. Arbegast W. Application of friction stir welding and related technology. In *Friction stir welding and Processing*, edited by R.S. Mishra & M.W. Mahoney. ASM International, Materials Park, OH, 2007. pp. 273-308.
  20. Nandan, R.; DebRoy, T. & Bhadeshia, H.K.D.H. Recent advances in friction-stir welding – Process, weldment structure and properties. *Prog. Mater. Sci.*, 2008, **53**(6), 980-1023. doi:10.1016/j.pmatsci.2008.05.001.
  21. Threadgill, P.L.; Leonard, A.J.; Shercliff, H.R. & Withers, P.J. Friction stir welding of aluminium alloys. *Int. Mater. Rev.*, 2009, **54**, 49-93. doi: 10.1179/174328009X411136
  22. Peng, Z. & Sheppard, T. Study of surface cracking during extrusion of aluminium alloy AA 2014. *Mater. Sci. Technol.*, 2004, **20**(9), 1179-1191. doi: 10.1179/026708304225022016.
  23. Thomas, W.M.; Nicholas, E.D.; Needham, J.C.; Murch, M.G.; Templesmith, P. & Dawes, C.J. Friction stir butt welding. USA patent 5460317, October 1995.
  24. Kumar, K. & Kailas, S.V. The role of FSW tool on material flow and weld formation. *Mater. Sci. Engg. A*, 2008, **485**(1-2), 367-374. doi: 10.1016/j.msea.2007.08.013.
  25. Colegrove, P.A.; Shercliff, H.R. & Zettler, R. Model for predicting heat generation and temperature in friction stir welding from the material properties. *Sci. Technol. of Weld. Join.*, 2007, **12**(4), 284-297. doi: 10.1179/174329307X197539.
  26. D'Urso, G.; Giardini, C.; Lorenzi, S. & Pastore, T. Fatigue crack growth in the welding nugget of FSW joints of a 6060 aluminum alloy. *J. Mater. Process. Technol.*, 2014, **214**(10), 2075-2084. doi: 10.1016/j.jmatprotec.2014.01.013.

#### ACKNOWLEDGEMENT

We express our gratitude to Defence Research and Development Organisation for the financial support to carry out this program. The authors are thankful to Dr S.V. Kamat, Director DMRL for his continued encouragement and support. We would like to thank all those who have either directly or indirectly extended their help in carrying out the studies.

#### CONTRIBUTORS

**Mr Suresh D. Meshram** received BE (Mechanical) from NIT, Surat, in 2000 and MTech (Prod. and Ind. System Engg.) from IIT Roorkee, in 2002. Currently pursuing his PhD from IIT Delhi. He is working as Scientist 'E' at Defence Metallurgical Research Laboratory (DMRL), Hyderabad. His area of research mainly includes joining of advance similar and dissimilar materials through process like electron beam welding, friction welding and friction stir welding and characterisation of welded joints.

**Dr G. Madhusudhan Reddy** obtained PhD in Metallurgical Engineering from Indian Institute of Technology, Madras in 1999. Presently as a Scientist 'H', he is heading the Metal Joining Group of DMRL, Hyderabad. He has more than 300 scientific publications to his credit. He is a Fellow of the Indian Welding Society and Institution of Engineers (India). Government of India recognised his contributions to the metallurgical sciences by the award 'Metallurgist of the Year'.

**Dr A Venugopal Rao** received PhD. in Mechanical Engineering from the Indian Institute of Technology Madras (IIT Madras). Presently as a Scientist 'F', he is heading the Modelling and Simulation Group at DMRL, Hyderabad. His research interests include : Computer aided engineering, fracture mechanics, workability analysis in metalworking, and continuum damage mechanics. He is also the Team Leader for Simulation in the DRDO project on *Development of Life Prediction Technologies for Aeroengine Components*. He has published over 20 papers in International and National journals.